

Random-phase surface-wave solitons in nonlocal nonlinear media

Assaf Barak,¹ Carmel Rotschild,¹ Barak Alfassi,¹ Mordechai Segev,¹ and Demetrios N. Christodoulides²

¹Physics Department and Solid State Institute, Technion, Haifa 32000, Israel

²College of Optics/CREOL, University of Central Florida, Florida 32816-2700, USA

Received June 8, 2007; accepted June 27, 2007;

posted July 16, 2007 (Doc. ID 83918); published August 10, 2007

We demonstrate, theoretically and experimentally, incoherent surface solitons in a noninstantaneous nonlocal nonlinear media. These incoherent surface waves are located at the interface between a nonlinear medium with long-range nonlocality and a linear dielectric medium (air). © 2007 Optical Society of America

OCIS codes: 190.0190, 190.4350, 190.6135, 240.6690.

Optical surface waves are waves localized at the boundary between two media with different properties. The unique properties of surface waves made them a topic of multidisciplinary research, from physics and material science to biology and engineering, promising applications for sensing, trapping, and imaging, with surface waves serving as tools for exploring the properties of material interfaces [1]. In linear optics, surface waves were identified on the interface between metals and dielectrics [2], at the boundary between a periodic (layered) structure and a homogeneous medium [3], or along the boundary between isotropic and anisotropic materials [4]. In the nonlinear domain, optical surface waves can exist at the interface between two media if at least one of them has nonlinear properties, whether the media are homogeneous [5–7] or periodic [8,9]. Surface waves were also observed in materials with nonlocal nonlinearities [10]. Here, we show that random-phase (spatially incoherent) surface-wave solitons can exist in noninstantaneous nonlocal nonlinear media.

Before proceeding, we revisit some aspects of incoherent solitons [11–14]. Since their discovery [11], incoherent solitons have been observed in various optical nonlinear media [13,15,16]. They were also studied in systems beyond optics, such as with matter waves [17], and spin waves [18]. Incoherent solitons were also found in nonlocal nonlinear media [19]. Combining the phenomena of surface waves and incoherent solitons raises the possibility of incoherent surface solitons. To explore this idea, we begin with the Helmholtz equation describing the propagation of monochromatic waves of frequency ω , in both media, nonlinear (medium 1) and linear (medium 2),

$$\nabla^2 E + k_0^2 n^2 E = 0. \quad (1)$$

An incoherent spatial soliton forms when a multimode beam, whose modal amplitudes vary randomly in time, induces (via a noninstantaneous nonlinearity) a multimode waveguide that traps the modes self-consistently [14]. In (1+1) dimensions, the field of an incoherent soliton is $E(x, z, t) = \sum_n c_n(t) u_n(x) \exp(i\Gamma_n z)$, where c_n is the modal amplitude that varies randomly with time, $u_n(x)$ is the normalized wave function of the n th mode, with Γ_n as its propagation constant. Substituting E into Eq. (1),

and separating into (mutually uncorrelated) modes, each mode obeys a Helmholtz equation in each medium separately, with the two equations connected through the boundary conditions at the interface. That is,

$$\frac{d^2 u_n(x)}{dx^2} + [k_0^2 (n_1^2 + 2n_1 \Delta n) - \Gamma_n^2] u_n(x) = 0, \quad (2a)$$

in the nonlinear medium, and

$$\frac{d^2 u_n(x)}{dx^2} + [k_0^2 n_2^2 - \Gamma_n^2] u_n(x) = 0, \quad (2b)$$

in the linear medium. n_1 and n_2 are the linear refractive indices in media 1,2, Δn is the nonlinear index change, and k_0 is the vacuum wavenumber. We are interested here in TE-polarized waves, for which the boundary conditions are continuities of $u_n(x)$ and $du_n(x)/dx$ at the interface. Each mode must fulfill the same boundary conditions. We seek solutions with spatial widths much smaller than the dimensions of the nonlinear medium, such that $u_n(x)$ and all its derivatives vanish at the other (far-away) interface. For a long-range nonlocal nonlinearity, this condition is important because boundaries exert forces even from afar [20]. Since the nonlinearity responds much slower than the typical fluctuation of $c_n(t)$, Δn depends only on the time-averaged intensity of the beam, $I = \langle |E|^2 \rangle = \sum_n d_n |u_n(x)|^2$, where $d_n = \langle |c_n|^2 \rangle$ are the modal weights (time-averaged populations) [14].

In nonlocal nonlinear media, the response at any point depends not only on the intensity at that point but also on the intensity within some nonlocality-range surrounding that point. Nonlocal optical nonlinearities have been found in various media, e.g., liquid crystals [15], semiconductor amplifiers [21], and thermal nonlinearities [22–24]. Nonlocal media tend to “average” effects of localized excitations. In spite of that, even long-range nonlocal nonlinear media can support solitons [24–27], which actually exhibit interaction properties [28,29] that are profoundly different than in local nonlinear media. In nonlinear media with a large nonlocality range, boundaries play a major role [10,20,24,29]: determining the shape of solitons (e.g., allowing the formation of elliptic solitons) [24], affecting the trajectories of solitons [20], and mediating interactions between solitons

propagating in different samples [29]. Finally, nonlocal nonlinearities support surface-wave solitons, which are self-trapped in the medium of a higher refractive index, and are attracted to the interface even when launched far away from it [10].

We proceed with the theory of incoherent surface waves in nonlocal nonlinear media. For concreteness, we analyze the case of the thermal nonlinearity of lead-glass [24], which is of the self-focusing type. The refractive index change, $\Delta n = \beta \Delta T$, is proportional to the temperature change, $\Delta T = T - T_0$, (T_0 being the temperature without light) induced by the optical intensity, where $\beta = dn/dT$ is the thermal coefficient of the refractive index. The propagating beam is slightly absorbed, which heats the glass. Under temporal steady-state conditions, the temperature change, ΔT , satisfies the heat equation, which is translated into a Poisson-type equation for Δn :

$$d^2 \Delta n(x)/dx^2 = -\gamma I(x), \quad (3)$$

where $\gamma = (\alpha\beta)/\kappa$, κ is the thermal conductivity and α is the absorption coefficient. In this medium, surface solitons occur at the proximity of thermally insulating boundaries [10]. Hence, we set $\partial T/\partial x = 0$ at the right (insulating) boundary, and $T = T_0$ at the left boundary, setting a fixed temperature there. These serve as boundary conditions for Eq. (3). We find incoherent surface solitons by solving Eqs. (2) together with Eq. (3) self-consistently (the numerical scheme is a combination of the methods of [14,24]). We use $n_1 = 1.8$, $\beta = 14 \times 10^{-6} \text{ K}^{-1}$, $\alpha = 0.01 \text{ cm}^{-1}$, $\lambda_0 = 488 \text{ nm}$, and $\kappa = 0.00637 \text{ [W K}^{-1} \text{ cm}^{-1}]$, with a sample of width 0.2 cm. The example shown in Fig. 1 depicts an incoherent surface soliton comprised of three modes of weights $d_1 = 0.8$, $d_2 = 0.15$, and $d_3 = 0.05$. Figures 1(a) and 1(c) show the normalized intensity distribution of the surface wave, $I(x)$, with $2.5 \times 10^5 \text{ [W/cm}^2]$ and $2.5 \times 10^7 \text{ [W/cm}^2]$ maximal intensity, respectively, together with the normalized $\Delta n(x)$. For a higher maximal intensity, the peak of the soliton is closer to the interface, and its width is smaller. Figure 1(b) shows

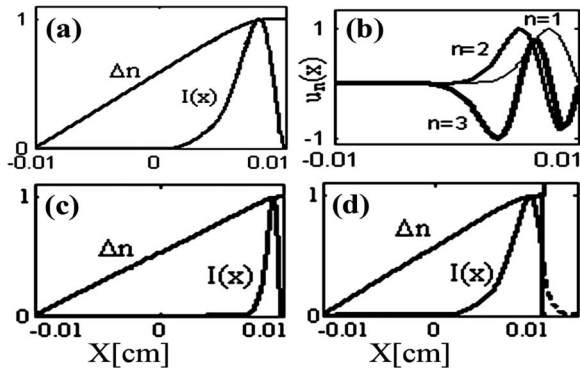


Fig. 1. Normalized intensity distribution, $I(x)$, of an incoherent surface soliton comprised of three modes of weights $d_1 = 0.8$, $d_2 = 0.15$, and $d_3 = 0.05$, and the induced index change, Δn , for $n_1 = 1.8$, $n_2 = 1$, at maximal intensity of (a) 2.5×10^5 and (c) $2.5 \times 10^7 \text{ [W/cm}^2]$. (b) Structures of the modes of the incoherent soliton shown in (a). (d) Incoherent surface soliton for $n_1 = 1.8$, $n_2 = 1.79998$, at maximal intensity of $2.5 \times 10^5 \text{ [W/cm}^2]$.

the structures of the three modal constituents of the incoherent soliton shown in Fig. 1(a). Figure 1(d) shows a surface soliton with $2.5 \times 10^5 \text{ [W/cm}^2]$ maximal intensity, when $n_1 - n_2$ is comparable to Δn . When the difference between the linear refractive indices, $n_1 - n_2$, is very large compared to Δn , most of the power of the surface soliton resides inside the nonlinear medium [Fig. 1(a)]. In contrast, when $n_1 - n_2$ is comparable to Δn , a sizable part of the soliton power is located in the linear medium [Fig. 1(d)]. We simulate the propagation of this surface soliton in the presence of initial random noise (amplitude and phase) up to 5% of the soliton intensity and find it stable over many diffraction lengths. We note that an incoherent surface soliton solution is uniquely defined by its total power and the power distribution among its modes. That is, given the material parameters, a soliton of a given power, distributed in some way among its modes, has only one solution, determining its shape, width, and the distance of its intensity peak from the interface.

Next, we study the propagation of high power beams when launched away from the surface. When one launches a coherent beam with the width and intensity needed for a surface soliton, off the soliton stable point, the beam oscillates instead of propagating on-axis [10]. Our simulations with incoherent beams show similar trends. Figure 2 shows an example for the soliton of Fig. 1(a). When the surface soliton is launched at its stable point, it propagates on-axis, maintaining its near interface trajectory [Fig. 2(a)]. Figure 2(b) depicts the same incoherent beam, launched $70 \mu\text{m}$ away from the stable point. The beam is initially pushed toward the interface by the optical force originating from the gradient in $\Delta n(x)$. Then the beam undergoes total internal reflection from the interface and moves back crossing the surface soliton stable point, after which it is pushed again toward the interface, bouncing from it again, etc.

Next, we describe the experiments, which are all carried in (2+1)D media. We use a quasi-monochromatic 488 nm laser beam and make it spatially incoherent by passing it through a rotating diffuser. We launch the beam into a lead-glass sample of dimensions $2 \text{ mm} \times 2 \text{ mm} \times 83 \text{ mm}$ (the latter being the propagation distance) with temperature boundary conditions $T(x, y = \pm d, z) = T(x = -d, y, z) = T_0$, and $\partial T(x = d, y, z)/\partial x = 0$ [Fig. 3(i)]. The time-averaged intensity FWHM of the input beam is $90 \mu\text{m}$, and its

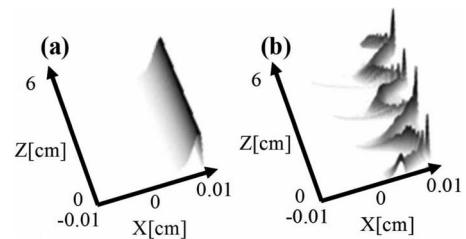


Fig. 2. Incoherent soliton of Fig. 1(a) (a) launched on its stable point and propagating on-axis, and (b) launched $70 \mu\text{m}$ away from the interface, exhibiting self-bouncing.

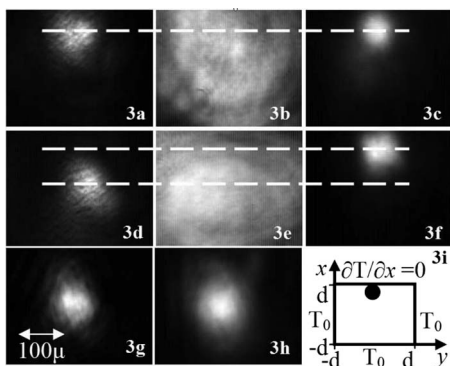


Fig. 3. Experimental photographs. (a) Incoherent input beam of $90\ \mu\text{m}$ FWHM and $30\ \mu\text{m}$ correlation distance launched near the interface. (b) At low power (100 mW) the beam broadens to $230\ \mu\text{m}$ FWHM output. (c) At 2.5 W the beam forms an incoherent surface soliton, exiting the sample with the same width and location as the input. (d) $90\ \mu\text{m}$ FWHM incoherent beam launched with its center $100\ \mu\text{m}$ away from the interface. (e) At low power (100 mW) the beam broadens to $230\ \mu\text{m}$ FWHM output, with its center $100\ \mu\text{m}$ away from the interface. (f) At 2.5 W the beam forms an incoherent surface soliton and is attracted to the interface, exiting the sample with a $90\ \mu\text{m}$ FWHM, and with its center $40\ \mu\text{m}$ away from the interface. (g) $90\ \mu\text{m}$ FWHM low power ($\sim 100\ \text{mW}$) spatially coherent beam launched near the interface, which (h) barely broadens within 8.3 cm propagation. (i) Cross section of the sample and temperature boundary conditions.

transverse correlation distance is $\sim 30\ \mu\text{m}$. First, we launch the incoherent beam close to the interface [Fig. 3(a)], with its center $40\ \mu\text{m}$ away from the interface. At low power ($\sim 100\ \text{mW}$), the beam broadens, exiting the sample with a $230\ \mu\text{m}$ FWHM [Fig. 3(b)], whereas at $\sim 2.5\ \text{W}$ the beam forms an incoherent surface soliton, exiting the sample with the same width and location as it enters [Fig. 3(c)]. We then launch the beam with its center $100\ \mu\text{m}$ away from the interface [Fig. 3(d)]. At low power the beam broadens as in Fig. 3(b), exiting the sample with its center shifted by $100\ \mu\text{m}$ from the interface [Fig. 3(e)]. However, at high power (2.5 W), the beam forms an incoherent surface soliton and is attracted to the interface, exiting with the same width as the input beam, but much closer to the interface [Fig. 3(f)]. The beam of Fig. 3(f) emerges at practically the same distance from the interface as the surface soliton shown in Fig. 3(c), which means the beam was displaced by $60\ \mu\text{m}$ from its launch point. The far-away boundary is pushing the incoherent beam toward the interface. Comparing the low-power behavior of the incoherent beam to that of a fully coherent beam of the same input width reveals a substantial difference. A low-power (100 mW) $90\ \mu\text{m}$ FWHM spatially-coherent beam launched at the proximity of the interface [Fig. 3(g)] barely broadens within 8.3 cm propagation [Fig. 3(h)], whereas an incoherent beam of the same width, having a correlation distance of $30\ \mu\text{m}$ broadens to $230\ \mu\text{m}$ [Figs. 3(b) and 3(e)].

In conclusion, we have demonstrated incoherent

surface solitons in nonlocal nonlinear media. The ideas developed here can be used to find TM-polarized incoherent surface solitons, (2+1)D incoherent surface solitons, and surface solitons residing primarily in the lower-index medium.

References

1. A. Zangwill, *Physics at Surfaces* (Cambridge U. Press, 1998).
2. V. M. Agranovich and D. L. Mills, *Surface Polaritons* (North-Holland, 1982).
3. P. Yeh, A. Yariv, and A. Y. Cho, *Appl. Phys. Lett.* **32**, 104 (1978).
4. D. Artigas and L. Torner, *Phys. Rev. Lett.* **94**, 013901 (2005).
5. W. Tomlinson, *Opt. Lett.* **5**, 323 (1980).
6. G. S. Garcia Quirino, J. J. Sanchez-Mondragon, and S. Stepanov, *Phys. Rev. A* **51**, 1571 (1995).
7. M. Cronin-Golomb, *Opt. Lett.* **20**, 2075 (1995).
8. K. G. Makris, S. Suntsov, D. N. Christodoulides, G. I. Stegeman, and A. Hache, *Opt. Lett.* **30**, 2466 (2005).
9. S. Suntsov, K. G. Makris, D. N. Christodoulides, G. I. Stegeman, A. Hache, R. Morandotti, H. Yang, G. Salamo, and M. Sorel, *Phys. Rev. Lett.* **96**, 063901 (2006).
10. B. Alfassi, C. Rotschild, O. Manela, M. Segev, and D. N. Christodoulides, *Phys. Rev. Lett.* **98**, 213901 (2007).
11. M. Mitchell, Z. Chen, M. F. Shih, and M. Segev, *Phys. Rev. Lett.* **77**, 490 (1996).
12. M. Mitchell and M. Segev, *Nature (London)* **387**, 880 (1997).
13. Z. Chen, M. Mitchell, M. Segev, T. H. Coskun, and D. N. Christodoulides, *Science* **280**, 889 (1998).
14. M. Mitchell, M. Segev, T. H. Coskun, and D. N. Christodoulides, *Phys. Rev. Lett.* **79**, 4990 (1997).
15. M. Peccianti and G. Assanto, *Opt. Lett.* **26**, 1791 (2001).
16. A. Picozzi, M. Haelterman, S. Pitois, and G. Millot, *Phys. Rev. Lett.* **92**, 143906 (2004).
17. H. Buljan, M. Segev, and A. Vardi, *Phys. Rev. Lett.* **95**, 180401 (2005).
18. M. Wu, P. Krivosik, B. A. Kalinikos, and C. E. Patton, *Phys. Rev. Lett.* **96**, 227202 (2006).
19. W. Krolikowski, O. Bang, and J. Wyller, *Phys. Rev. E* **70**, 036617 (2004).
20. B. Alfassi, C. Rotschild, O. Manela, M. Segev, and D. N. Christodoulides, *Opt. Lett.* **32**, 154 (2007).
21. E. A. Ultanir, G. I. Stegeman, D. Michaelis, C. H. Lange, and F. Lederer, *Phys. Rev. Lett.* **90**, 253903 (2003).
22. A. Dreischuh, D. N. Neshev, D. E. Petersen, O. Bang, and W. Krolikowski, *Phys. Rev. Lett.* **96**, 043901 (2006).
23. F. W. Dabby and J. R. Whinnery, *Appl. Phys. Lett.* **13**, 284 (1968).
24. C. Rotschild, O. Cohen, O. Manela, M. Segev, and T. Carmon, *Phys. Rev. Lett.* **95**, 213904 (2005).
25. S. K. Turitsyn, *Theor. Math. Phys.* **65**, 797 (1986).
26. C. Conti, M. Peccianti, and G. Assanto, *Phys. Rev. Lett.* **91**, 73901 (2003).
27. W. Krolikowski, O. Bang, N. I. Nikolov, D. Neshev, J. Wyller, J. J. Rasmussen, and D. Edmundson, *J. Opt. B: Quantum Semiclassical Opt.* **6**, S288 (2004).
28. N. I. Nikolov, D. Neshev, W. Krolikowski, O. Bang, J. J. Rasmussen, and P. L. Christiansen, *Opt. Lett.* **29**, 286 (2004).
29. C. Rotschild, B. Alfassi, O. Cohen, and M. Segev, *Nat. Phys.* **2**, 769 (2006).